The Effects of H_2O_2 Concentration on Formation of Uranyl Peroxide Species Probed by Dissolution of Uranium Nitride and Uranium Dioxide

Sarah Hickam,[a] Jaclyn Breier,[a] Yasmeen Cripe,[a] Erica Cole,[a] Peter C. Burns[a,b]

[a]Department of Civil and Environmental Engineering and Earth Sciences, University of Notre Dame, Notre Dame, Indiana 46556, United States

[b]Department of Chemistry and Biochemistry, University of Notre Dame, Notre Dame, Indiana 46556, United States

[*]To whom correspondence should be addressed. Email: pburns@nd.edu

ABSTRACT: Dissolution of uranium materials in alkaline aqueous conditions containing H_2O_2 results in uranyl peroxide species in solution, including anionic uranyl peroxide cage clusters. Uranyl peroxide cage clusters are generally highly soluble in water, where they persist as aqueous macroanions. Previous studies indicate that uranyl cluster speciation and dissolution of uranium materials is impacted by the concentration of alkali metal in solution, but in these studies, high concentrations of H_2O_2 were used. Herein, the role of hydrogen peroxide concentration is examined relative to the dissolution of powdered UN and UO_2. Lower initial H_2O_2 concentrations reduce dissolution of UO_2 and UN and tend to produce simple (small) uranyl peroxide species rather the highly soluble uranyl peroxide clusters. H_2O_2 availability will have implications for uranyl speciation and solubility where spent nuclear fuel is in contact with water and where alkaline peroxide conditions are used in dissolution of nuclear material.

INTRODUCTION

Metal oxide clusters including transition metal and actinide polyoxometalates (POMs) are typically synthesized using soluble precursor materials;[1] however, recent studies have focused on using uranyl peroxide cluster-forming conditions to dissolve UO_2 solid, which is sparingly soluble in non-oxidizing conditions.[2-3] During dissolution, peroxide oxidizes U^{IV} to U^{VI} and hydrolysis reactions release uranyl ions to solution. The presence of alkali metals in addition to H_2O_2 can result in aqueous uranyl peroxide cage clusters, with alkali concentration correlated with dissolved U concentrations.[3]

Typical transition metal oxide clusters contain metal atoms and oxo bridges, with strongly bound *yl* O atoms or organic ligands passivating the outside of clusters.[4] Additional ligands, such as pyrophosphate and oxalate, may be incorporated as bridges between metal centers in the cage structures.[4-6] In the case of uranyl peroxide clusters, U-O_2-U (peroxide) bridges are essential for formation (Figure 1). Synthesis of uranyl peroxide clusters typically involves 10 to 20 times more moles of H_2O_2 relative to the respective uranium concentrations, although syntheses with as low as two [7] and as high as 30 [8-9] times the molar concentration of H_2O_2 to U have been described.[4, 9-21]

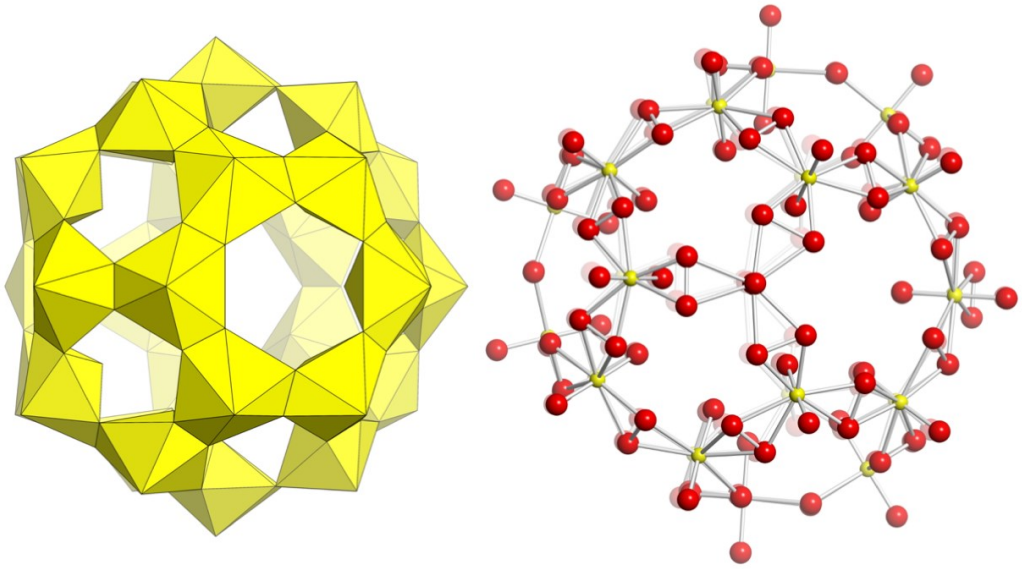

Figure 1. Polyhedral (left) and ball and stick (right) representations of the uranyl peroxide cluster $[(UO_2)_{28}(O_2)_{42}]^{28-}$ (U_{28}). Countercations and water molecules are omitted. Uranium polyhedra and atoms are shown in yellow, with oxygen atoms shown as red balls.

Experiments and simulations intended to improve understanding of the properties and formation mechanisms of uranyl peroxide cage clusters have examined the influence of alkali counter cations, pH, and bridging ligands.[3, 11, 13, 22-25] However, H_2O_2 is critical for the formation of these clusters and limited availability will impact cluster formation; thus, studies of the action of H_2O_2 in different concentrations on uranium solids may provide insights relative to cluster formation requirements and mechanisms. Additionally, peroxide concentrations have implications for uranium reprocessing and recovery schemes that utilize H_2O_2 [26-28] and may also influence the fate of uranium where alpha radiolysis of water leads to peroxide formation, such as where water interacts with nuclear waste.[29-33] During dissolution of low-valent uranium materials such as $U^{III}N$ and $U^{IV}O_2$ in uranyl peroxide cluster-forming conditions, peroxide is necessary to promote the oxidation of U to $(UO_2)^{2+}$ ions, and thus, available peroxide has additional importance. The purpose of this study is to explore the effects of H_2O_2 concentration on the extent of dissolution of uranium-based materials such as UN and UO_2 in alkaline

conditions and characterize the resulting uranyl solution species. The use of unirradiated UN and UO_2 here presents a starting point for studies of these materials in cluster-forming conditions, as additional variables will need to be considered for studies of surrogate or irradiated spent nuclear fuel including complex and heterogeneous chemical compositions and intense radiation fields.

EXPERIMENTAL SECTION

Dissolution Experiments. Uranium nitride (UN) was synthesized and characterized at Los Alamos National Laboratory (Supporting Information). UN is pyrophoric so dissolution experiments were conducted in an Ar inert atmosphere glovebox. UN was ground with a mortar and pestle to a powder and weighed into Teflon vials. Due to the limited quantity of material available and based on preliminary experiments, the mass of UN used in each experiment ranged from 7.5 to 85 mg and UN was not completely dissolved during any experiment. Hydrogen peroxide and LiOH solutions were added to vials containing UN. For H_2O_2, 200 μL of 30% (9.8 M) H_2O_2 or H_2O_2 diluted to 0.5, 1, 3, or 5 M concentration was added directly to vials containing UN. A 2.38 M LiOH solution was then added, in volumes of 9.5, 27.5, 54.0, or 114 μL, corresponding to LiOH concentrations in the system of 0.1, 0.3, 0.5, or 0.9 M, respectively.

Each set of dissolution conditions was repeated three times. Experiments were allowed to react for several minutes until bubbling ceased and then were capped and parafilmed. Aliquots of solutions were taken periodically for elemental analysis to determine steady state elemental concentrations. Solution pH measurements were taken on the last day of experiments, which was at least three days after initial dissolution. Experiments were likewise

conducted using UO_2 powders. Additionally, UN was dissolved in aqueous solutions containing LiOH or H_2O_2 alone (Supporting Information, Table S1).

Inductively Coupled Plasma Optical Emission Spectrometry. Aliquots of solutions from dissolution experiments were centrifuged and then diluted with 18 mΩ water. 70% nitric acid was added to the solutions to give a concentration of 5% HNO_3 and then yttrium was added as an internal standard. Each experiment had three separate dilutions as replicates for elemental analysis. Samples were analyzed for U and Li by a PerkinElmer Optima 8000 inductively coupled plasma optical emission spectrometer (ICP-OES), and concentrations of each element were calculated from a calibration curve derived from ten standards. Measured concentrations are given in moles/kg solution and parts per million (ppm), as all dilutions were measured gravimetrically and solutions have varying densities. The average concentration from multiple dilutions was averaged with the dissolution condition replicates to provide U and Li concentrations for each experimental condition.

Raman Spectroscopy. Raman spectra of solutions were acquired using a Renishaw inVia confocal microscope system equipped with a 785 nm laser. The laser power at the sample was attenuated to approximately 96 mW.

Electrospray Ionization Mass Spectrometry. Centrifuged aliquots of solutions from dissolution experiments were diluted in 18 mΩ water to concentrations of ~1000 ppm U and were injected at 600 μL/hour into a Bruker micrOTOF-Q II high-resolution quadrupole time of flight

spectrometer operating in negative ion mode. Instrument parameters included a 3000 capillary voltage, 0.85 bar nebulizer, and 4 L/min dry gas. Data were collected over 2.5 minutes in the 500 to 5000 m/z region.

Powder X-ray Diffraction. Uranium nitride starting material was characterized by powder X-ray diffraction using a Bruker D2 Phaser diffractometer with Bragg-Brentano geometry and Ni-filtered Cu Kα radiation. The samples were hermetically sealed in a sample holder within an Ar atmosphere to eliminate oxygen contamination prior to X-ray diffraction analysis. Solids remaining after dissolution experiments were pressed onto a glass slide and analyzed with a Bruker D8 Advance diffractometer with Cu Kα radiation.

RESULTS AND DISCUSSION

Uranium nitride and uranium dioxide dissolution in aqueous solutions containing hydrogen peroxide and LiOH is extensive and rapid. Steady state is typically reached within one hour of the combination of reactants for all starting concentrations of LiOH (Supporting Information, Figure S2). The dissolution reaction is accompanied by the evolution of O_2 gas, which is generally consistent with formation of nanoscale uranyl peroxide clusters.[23,34] Nitrogen gas release was not significant for UN dissolution (Supporting Information), indicating that most nitrogen remained in solution. Raman spectra show the presence of nitrate ions, and the presence of ammonium ions, although not detected, would be consistent with dissolution of transition metal nitrides with H_2O_2 (Supporting Information).[35, 36] Secondary phases were observed, including studtite (Supporting Information).

Dissolution of UN in solutions with different LiOH concentrations

Solutions containing different concentrations of LiOH were used to probe the impact of counter cation concentration and pH on UN dissolution for comparisons with UO_2. Adding 200 μL of 9.8 M H_2O_2 to the reactants yielded a linear correlation between measured concentrations of Li and U in solution for all LiOH concentrations (Figure 2), consistent with dissolution of UO_2 in similar conditions.[3] For UO_2 dissolution, a molar ratio of Li to U of 1 was observed, but UN dissolution exhibits an average ratio of 0.87 ± 0.11. The pH of solutions ranged from 6.39 ± 0.12 to 9.91 ± 0.29 and nonlinearly increased with Li concentration, with the largest increase in pH for the 0.9 M LiOH experiments. Vibrational modes in Raman spectra for these solutions between 800 and 850 cm^{-1} (Figure 3) and broad peaks in ESI-MS (Figure 4) indicate that uranyl peroxide clusters formed during dissolution of UN.

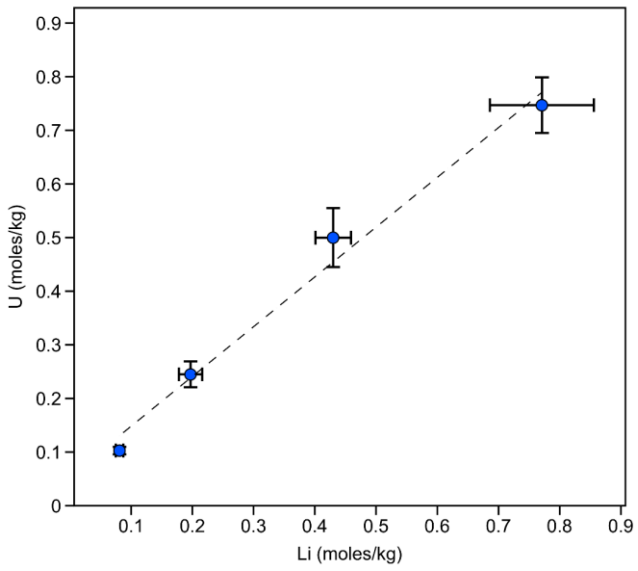

Figure 2. Concentration of Li versus concentration of U, in moles per kg of solution, resulting from dissolution of UN using 9.8 M H_2O_2. Error bars represent standard deviation of replicates. The dashed line is the linear correlation of Li and U concentrations measured in solution, where y= 0.9267x +0.0564 (R^2 = 0.9855).

Raman spectra of solutions collected from UN dissolution experiments that had 200 μL of 9.8 M H_2O_2 contain modes around 875 cm^{-1} indicating free peroxide[37] for starting LiOH concentrations below 0.3 M (Figure 3). Raman shifts in these spectra for uranyl and uranyl-bridging peroxo ligands are at 806 and 830 cm^{-1} respectively, indicating uranyl peroxide clusters with only peroxide bridges between uranyl ions (such as U_{20} or U_{28}).[3] Corresponding ESI-MS spectra (Figure 4) indicate species masses of 9.0 kDa. These data are consistent with $Li_{28}[(UO_2)_{28}(O_2)_{42}]$ (Li-U_{28}) clusters in solution.[3]

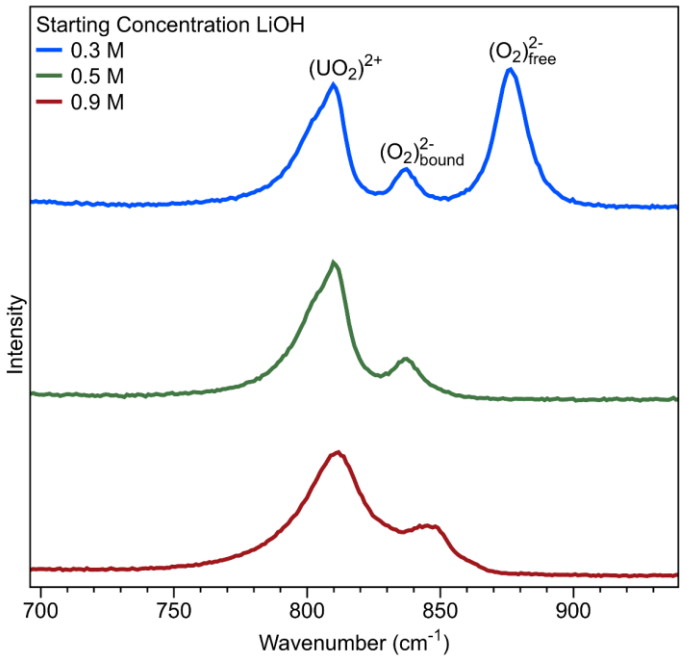

Figure 3. Raman spectra of solutions resulting from dissolution of UN in solutions containing 200 μL of 9.8 M H_2O_2 with increasing LiOH concentrations from top to bottom.

Analogous to dissolution of UO_2 under similar aqueous conditions,[3] dissolution of UN in solutions with higher LiOH concentrations results in polydisperse systems. ESI-MS spectra of solutions with starting LiOH concentrations greater than 0.3 M reflect the presence of multiple

clusters, including U_{28} (Figure 4). These solutions do not contain free peroxide according to the Raman spectra.

Uranyl peroxide cage clusters containing only peroxide and hydroxyl ligands carry a negative charge with absolute value equal to the number of uranium atoms in the cluster.[5] Smaller uranyl peroxide species, such as the monomer $[(UO_2)(O_2)_3]^{4-}$, carry higher charges.[38,39] The observed range of Li:U molar ratios and characteristic cluster signals in Raman and ESI-MS spectra are consistent with most of the uranium occurring in cage clusters (i.e. ~1), rather than highly negatively charged uranyl species. However, marginally lower Li:U molar ratios from dissolution of UN relative to UO_2 indicate that nitrogen species, such as ammonium ions, which can be incorporated as countercations in cluster structures, may be present.[11]

The maximum concentration of U in solution under this set of experimental conditions (i.e. 200 μL of 9.8 M H_2O_2 and various LiOH concentrations) is limited by the availability of Li countercations to form uranyl peroxide clusters, as indicated by the linear trend in Figure 2, and not by the cluster species or the pH values. However, it is notable that the increasing complexity of the ESI-MS spectra at higher LiOH concentrations corresponds to elimination of free peroxide in solution as indicated by the Raman spectra; thus, UN and UO_2 dissolution experiments using different initial H_2O_2 concentrations were used to probe the effect of available peroxide on dissolution and speciation.

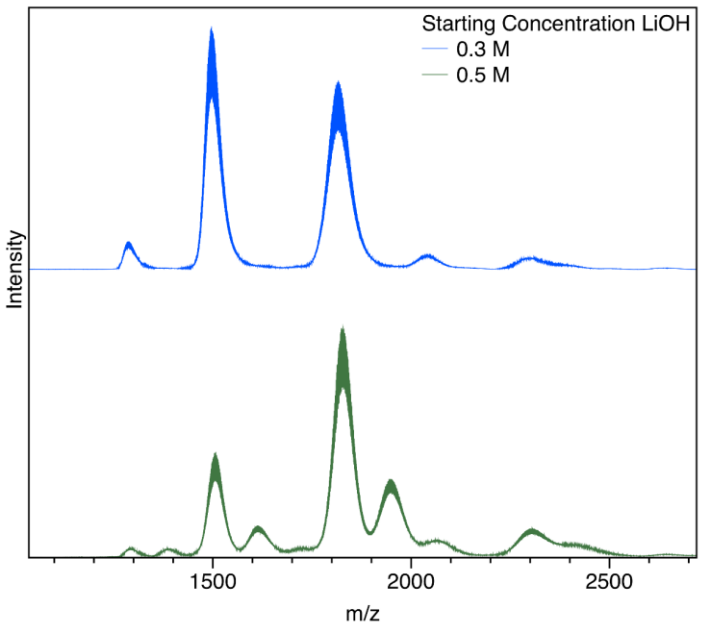

Figure 4. ESI-MS spectra of UN dissolution in a solution with 200 μL of 9.8 M H_2O_2 showing typical peak envelopes for $Li_{28}[(UO_2)_{28}(O_2)_{42}]$ (Li-U_{28}) at 0.3 M LiOH added and additional peaks at higher concentrations of LiOH.

Dissolution of UN in solutions with different H_2O_2 concentrations

The concentrations of U resulting from UN dissolution in aqueous solutions that had various initial H_2O_2 concentrations and four different LiOH concentrations are shown in Figure 5 and Figure 6. For 200 μl of H_2O_2 added with concentrations ranging from 1 to 9.8 M and the lowest starting LiOH concentrations of 0.1 M (H_2O_2:Li = 8.8 to 86), UN dissolution yields U concentrations of 2.07 to 2.67 x 10^4 ppm (0.087 to 0.112 mol U/kg sample). These concentrations correspond to measured Li:U molar ratios ranging from 0.77 to 1.04 (Supporting Information, Table S2). Concentrations of U in solution to which 200 μL of 3 M and higher H_2O_2 was added are statistically indistinguishable, with similar Li:U molar ratios, indicating that available Li to form uranyl peroxide clusters limits the extent of UN dissolution and smaller species that would carry higher negative charges were not formed. Overall, for 0.1 M LiOH

experiments, the H_2O_2 concentrations studied did not appreciably affect U dissolution or uranyl peroxide cluster assembly relative to 9.8 M H_2O_2 experiments.

For the next, higher initial LiOH concentration studied, 0.3 M, dissolution of UN in a solution to which 200 μL of 1 M H_2O_2 added (H_2O_2:LiOH=3.48) resulted in a U concentration distinctly lower than those to which 200 μL of 3 to 9.8 M H_2O_2 (H_2O_2:LiOH greater than 9.1) was added (0.127 mol U/kg of solution versus 0.245-0.275 mol U/kg of solution), indicating that peroxide availability is important (Figure 5, top right). Further increasing LiOH concentrations to 0.5 M reveals that 200 μL of 0.5 to 1 M H_2O_2 added (H_2O_2:LiOH=0.78-1.98) results in significantly lower U concentrations as compared to those with 200 μL of 3 to 9.8 M H_2O_2 (H_2O_2:LiOH>4.67) (Figure 5, bottom left). A more pronounced trend is observed for 0.9 M LiOH starting concentrations (H_2O_2:LiOH=0.37-7.22), where the resulting U concentrations upon dissolution of UN decreased with decreasing H_2O_2 concentration (Figure 5, bottom right). Generally, starting ratios of H_2O_2:LiOH less than 4:1 led to significantly lower U concentrations relative to 200 μL of 9.8 M H_2O_2 experiments .

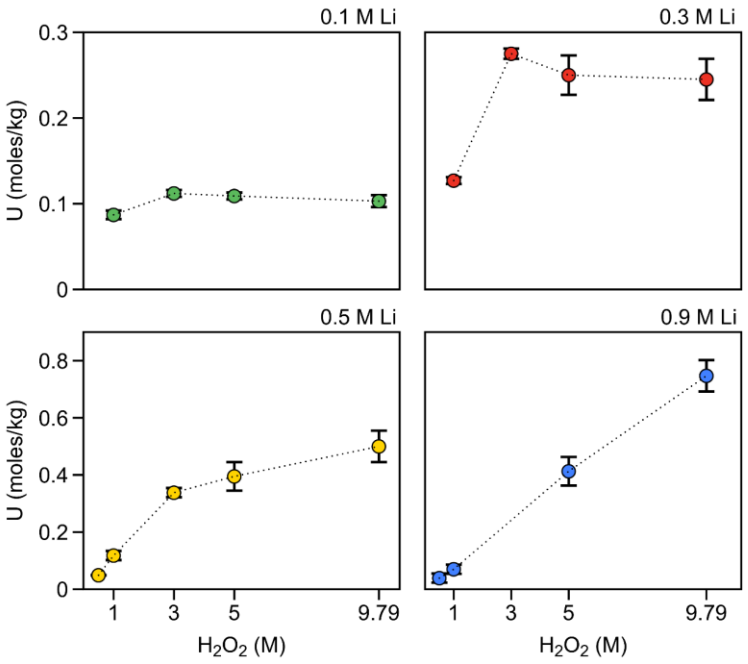

Figure 5. Concentration of 200 µL H_2O_2 added to each dissolution experiment versus concentration of U from dissolution of UN with H_2O_2 and 0.1, 0.3, 0.5, or 0.9 M LiOH. Error bars represent standard deviation of replicates.

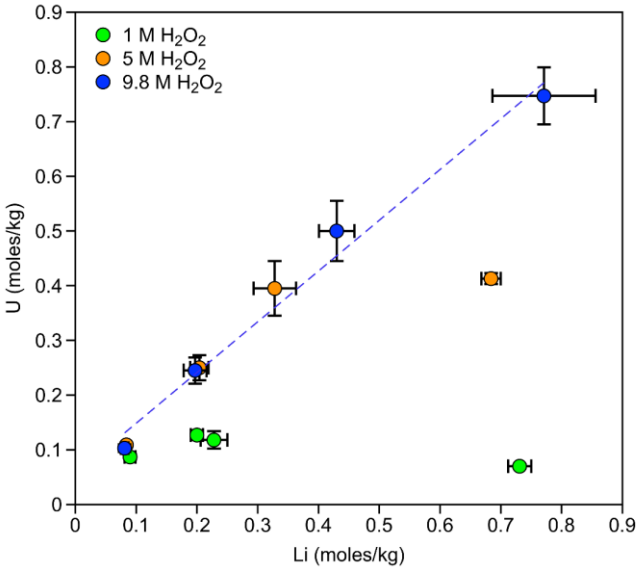

Figure 6. Concentration of Li versus U measured by ICP-OES for 200 µL 1 M, 5 M, and 9.8 M H_2O_2 addition experiments. The correlation between Li and U for 200 µL 9.8 M H_2O_2 experiments is shown by the dashed line. Standard deviation of replicates is shown as error bars.

Figure 6 shows the concentrations of Li and U measured in solutions resulting from dissolution of UN for which 200 µL of 1 M, 5 M, or 9.8 M H_2O_2 was added with variable LiOH

concentrations. For dissolution of UN in solutions containing a specific amount of LiOH, the measured Li concentrations were within error of each other regardless of H_2O_2 concentration, except for the experiments with 0.5 M LiOH. The targeted and measured Li concentrations are provided in the Supporting Information, Table S3, and exhibit differences for all experiments.

The experiments with 200 μL of 1 M H_2O_2 did not yield Li and U values consistent with the trend observed for experiments to which 200 μL of 9.8 M H_2O_2 was added (Figure 6). Instead, for solutions containing greater than 0.3 M LiOH, a slightly negative trend of U concentration with increasing Li concentration is evident. For experiments with 200 μL of 5 M H_2O_2, U concentrations follow the linear trend observed for experiments containing 200 μL of 9.8 M H_2O_2 until the highest LiOH concentrations added (0.9 M). Experiments with 200 μL of 1 M and or 5 M H_2O_2 that are inconsistent with the trend for experiments with 200 μL of 9.8 M H_2O_2 have Li:U ratios greater than one (Supporting Information, Table S2), which is consistent with the presence of uranyl species in solution with higher charges per uranium than unity.

Spectroscopic characterization of solutions resulting from UN dissolution seven days after commencement of the reactions indicated that uranyl peroxide clusters formed in almost all experimental conditions, including those with high Li:U ratios. However, characterization of solutions immediately after the dissolution reactions began reveals that the initial uranyl species in solutions with high Li:U ratios are not uranyl peroxide cage clusters. For example, for experiments done with 200 μL of 1 M H_2O_2 and 0.9 M Li added, for which the measured Li:U ratio was 10.4, Raman spectra acquired within minutes of UN dissolution and again 12 hours later contain a broad peak at approximately 700 cm^{-1} (Figure 7). This vibrational mode in combination with those between 800 and 850 cm^{-1} is characteristic of uranyl peroxide

monomer species, $[(UO_2)(O_2)_3]^{4-}$.[38-39] Corresponding ESI-MS spectra after 12 hours show weak broad signals in the 500 to 2500 m/z region (Figure 8). After six days, these signals are more intense relative to the background and the broad band at 700 cm^{-1} in the Raman spectra is absent, indicating uranyl peroxide cluster assembly. The observation of clusters in a solution that originally contained uranyl triperoxide monomers is consistent with a previous study in which reactions had high ratios of alkali to uranium.[11]

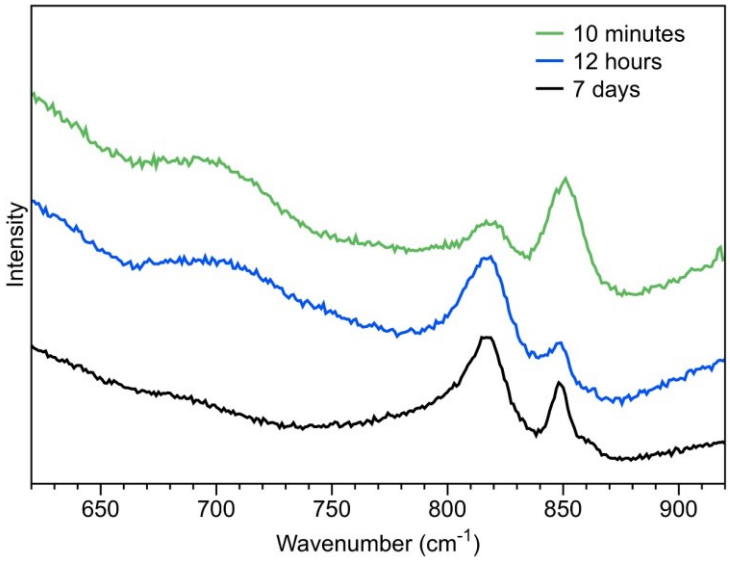

Figure 7. Raman spectra from UN dissolution in aqueous solutions containing 200 μL of 1 M H_2O_2 and 0.9 M LiOH minutes to days after reaction.

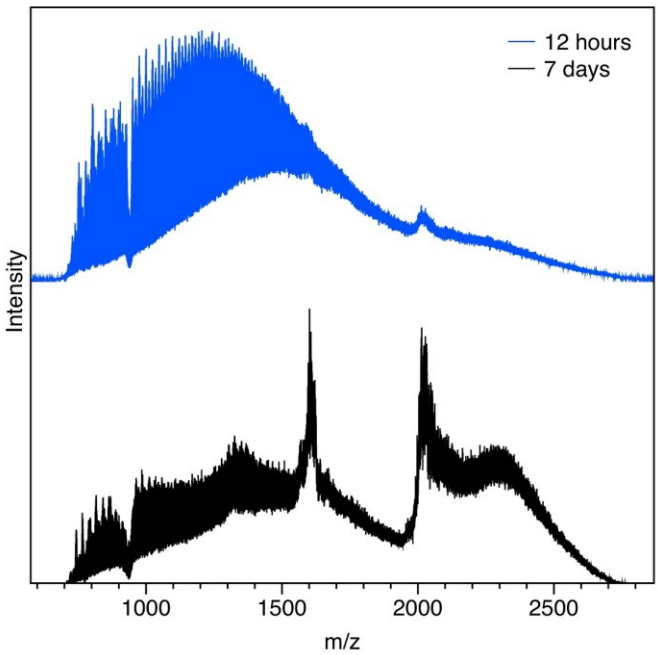

Figure 8. ESI-MS of UN dissolution reactions with 200 μL of 1 M H_2O_2 and 0.9 M Li after 12 hours and 7 days.

In the case of addition of 200 μL of 5 M H_2O_2 and 0.9 M Li, which gave an average Li:U ratio of 1.66, the Raman spectrum collected five minutes after the initial reaction commenced (Figure 9) has a broad shoulder centered around 760 cm^{-1}. This indicates uranyl peroxide cluster precursor motifs such as pentamers or tetramers of uranyl ions bridged by peroxide (Figure 10) may be present in addition to uranyl peroxide clusters. However, this shoulder disappears within 12 hours, at which time only signals typical of uranyl peroxide clusters in the region between 800 to 850 cm^{-1} remain.

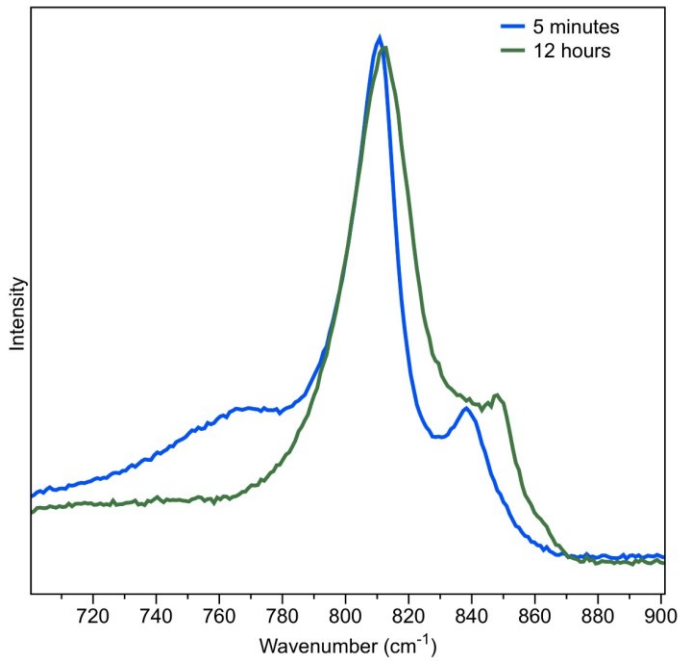

Figure 9. Raman spectra of 0.9 M Li UN dissolution experiment solutions with 200 μL of 5 M H_2O_2 after 5 minutes and 12 hours.

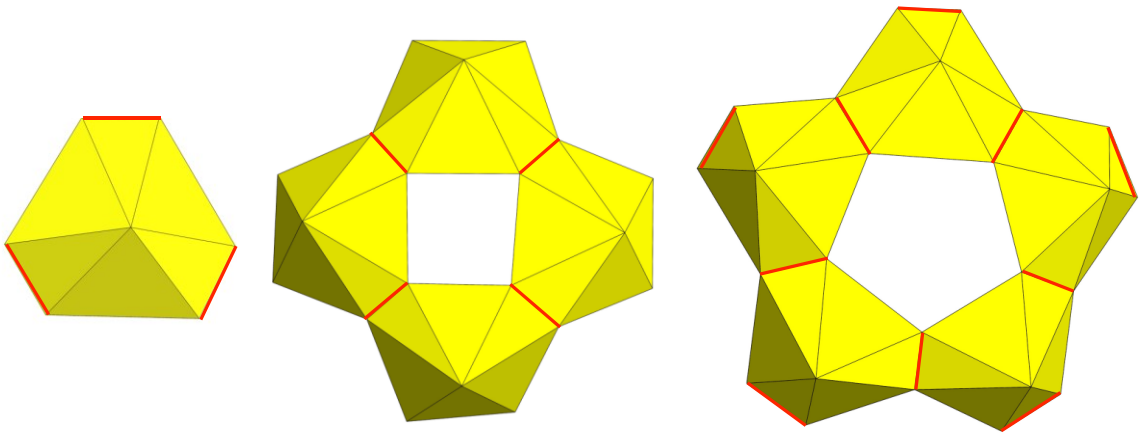

Figure 10. Polyhedral representations of uranyl peroxide-based monomers, tetramers, and pentamers. Peroxo ligands are indicated by red lines.

Raman spectra acquired minutes after commencement of UN dissolution for aforementioned experiments with solution Li:U ratios greater than 1 indicate the presence of monomeric and other uranyl peroxide cluster building blocks, but do not contain the free peroxide vibrational mode. In most cases, peaks with wavenumbers less than 800 cm^{-1} are not

observed in spectra collected after several hours or days, indicating that clusters assemble or become the dominant species over time. For experiments that had 200 μL of 0.5 M H_2O_2 added, Raman modes attributable to clusters were not evident in spectra collected after seven days. The time required for cluster assembly as well as the identity of the uranyl peroxide species formed depends on the quantity of H_2O_2 added, where lower peroxide concentrations favored smaller uranyl peroxide species and delayed cluster assembly. Overall, these solutions have high Li:U ratios and average pH values of 12.40 ± 0.60 (Supporting Information, Table S2 and Table S4). In contrast, experiments with Li:U ratios of approximately one had average solution pH values of 8.08 ± 1.30. The initial molar ratios of H_2O_2 to LiOH in dissolution experiments that resulted in the lower U concentrations and high Li:U ratios were generally less than 4:1.

UO_2 dissolution with different H_2O_2 and alkali hydroxide concentrations

Experiments were also done to examine dissolution of powdered UO_2 in solutions containing LiOH, NaOH, and KOH. The previous study of UO_2 dissolution with different alkali cation concentrations and 9.8 M hydrogen peroxide revealed that alkali metal identity was significant for cluster speciation and the maximum U concentrations that could be obtained by dissolution.[3] As for the UN dissolution experiments, the concentration and speciation of U in solution from UO_2 dissolution with H_2O_2 and alkali hydroxide depended on H_2O_2 concentration. At 0.9 M Li added and 200 μL of 0.5 M H_2O_2, uranyl peroxide monomers were also indicated by Raman spectra where UO_2 was the starting material. For NaOH, low concentrations of H_2O_2 also led to the formation of uranyl peroxide monomer species. For KOH systems, uranyl peroxide

monomers were not detected in solution after seven days under the conditions studied, but K:U ratios and U concentrations were affected by low H_2O_2 concentrations.

CONCLUSIONS

The concentration of initial H_2O_2 relative to alkali metal concentrations is an important factor in the extent of dissolution of U materials in alkaline peroxide systems. For dissolution of UN and UO_2 powders in alkaline solutions in the current study, the role of peroxide is to (1) oxidize uranium and (2) bind to U centers to form uranyl peroxide species. The findings of this study show that alkali concentrations in solution determine dissolution only if the starting conditions include sufficient H_2O_2. Specifically, initial molar concentrations of H_2O_2 that are equal to or exceed the concentration of LiOH by approximately 4:1 H_2O_2:LiOH result in highest dissolved U in solution. Decreasing the starting H_2O_2:LiOH ratio to less than 4:1 results in diminished dissolution of U likely due to changes in solution speciation as revealed by the combination of ESI-MS and Raman spectroscopy.

Limited dissolution of UN and UO_2 at low relative H_2O_2 concentrations coincides with observations of simpler (smaller and higher charged per uranium) uranyl peroxide species such as $[UO_2(O_2)_3]^{4-}$, $[(UO_2(O_2)_2)_4]^{8-}$ or $[(UO_2(O_2)_2)_5]^{10-}$ in the solutions. These monomeric and oligomeric species are readily detected in the hours after dissolution and over time and, as uranyl peroxide clusters assemble in these high pH conditions, their relative abundance in solution decreases. Therefore, uranyl speciation during dissolution with alkali hydroxide and H_2O_2 must be considered. The present study demonstrates that dissolution of low valent, nuclear fuel-like materials is most efficient when the concentration of H_2O_2 is maintained at, or

above four times the concentration of the alkali hydroxide resulting in formation of highly soluble, negatively charged uranyl peroxide clusters such as $[(UO_2)_{28}(O_2)_{42}]^{28-}$. The high concentrations of U achieved in neutral to alkaline pH conditions here present an alternative to current reprocessing schemes using hot nitric acid.

This study is the first that probes H_2O_2 availability as a factor in uranyl peroxide cluster formation, but quantifying the concentrations of H_2O_2 needed to form clusters under typical synthetic conditions will require additional studies, as dissolution of the low valent materials here requires additional H_2O_2 to oxidize U. Future experiments using U^{VI} materials and variable H_2O_2 may provide significant insight into formation mechanisms of uranyl peroxide clusters.

ACKNOWLEDGMENTS

This research was supported by the Department of Energy, National Nuclear Security Administration under Award Number DE-NA0003763. The authors thank Dr. Adam J. Parkison at Los Alamos National Laboratory for providing uranium nitride and for interesting discussions regarding the synthesis process. We also thank Dr. Ian V. Lightcap for assisting with GC-MS analyses. Additionally, we thank the Materials Characterization Facility, the Mass Spectrometry and Proteomics Facility, and the Center for Environmental Science and Technology at the University of Notre Dame for instrumentation used in this work.

REFERENCES

(1) Miras, H. N.; Yan, J.; Long, D. L.; Cronin, L., Engineering polyoxometalates with emergent properties. *Chem. Soc. Rev.* **2012,** *41*, 7403-7430.

(2) Wylie, E. M.; Peruski, K. M.; Prizio, S. E.; Bridges, A. N. A.; Rudisill, T. S.; Hobbs, D. T.; Phillip, W. A.; Burns, P. C., Processing used nuclear fuel with nanoscale control of uranium and ultrafiltration. *J. Nucl. Mater.* **2016,** *473*, 125-130.
(3) Hickam, S.; Aksenov, S. M.; Dembowski, M.; Perry, S. N.; Traustason, H.; Russell, M.; Burns, P. C., Complexity of uranyl peroxide cluster speciation from alkali-directed oxidative dissolution of uranium dioxide. *Inorg. Chem.* **2018,** *57*, 9296-9305.
(4) Nyman, M.; Burns, P. C., A comprehensive comparison of transition-metal and actinyl polyoxometalates. *Chem. Soc. Rev.* **2012,** *41*, 7354-7367.
(5) Qiu, J.; Burns, P. C., Clusters of actinides with oxide, peroxide, or hydroxide Bridges. *Chem. Rev.* **2013,** *113*, 1097-1120.
(6) Hickam, S.; Burns, P. C., Oxo Clusters of 5f Elements. In *Recent Development in Clusters of Rare Earths and Actinides: Chemistry and Materials*, Zheng, Z., Ed. Springer Berlin Heidelberg: Berlin, Heidelberg, 2017; pp 121-153.
(7) Unruh, D. K.; Burtner, A.; Pressprich, L.; Sigmon, G. E.; Burns, P. C., Uranyl peroxide closed clusters containing topological squares. *Dalton Trans.* **2010,** *39*, 5807-5813.
(8) Sigmon, G. E.; Unruh, D. K.; Ling, J.; Weaver, B.; Ward, M.; Pressprich, L.; Simonetti, A.; Burns, P. C., Symmetry versus minimal pentagonal adjacencies in uranium-based polyoxometalate fullerene topologies. *Angew. Chem. Int. Ed.* **2009,** *48*, 2737-2740.
(9) Nyman, M.; Rodriguez, M. A.; Alam, T. M., The U_{28} nanosphere: what's inside? *Eur. J. Inorg. Chem.* **2011,** 2197-2205.
(10) Burns, P. C.; Kubatko, K. A.; Sigmon, G.; Fryer, B. J.; Gagnon, J. E.; Antonio, M. R.; Soderholm, L., Actinyl peroxide nanospheres. *Angew. Chem. Int. Ed.* **2005,** *44*, 2135-2139.
(11) Falaise, C.; Nyman, M., The key role of U_{28} in the aqueous self-assembly of uranyl peroxide nanocages. *Chem.-Eur. J.* **2016,** *22*, 14678-14687.
(12) Qiu, J.; Dembowski, M.; Szymanowski, J. E. S.; Toh, W. C.; Burns, P. C., Time-resolved X-ray scattering and Raman spectroscopic studies of formation of a uranium-vanadium-phosphorus-peroxide cage cluster. *Inorg. Chem.* **2016,** *55*, 7061-7067.
(13) Liao, Z. L.; Ling, J.; Reinke, L. R.; Szymanowski, J. E. S.; Sigmon, G. E.; Burns, P. C., Cage clusters built from uranyl ions bridged through peroxo and 1-hydroxyethane-1,1-diphosphonic acid ligands. *Dalton Trans.* **2013,** *42*, 6793-6802.
(14) Qiu, J.; Ling, J.; Sui, A.; Szymanowski, J. E. S.; Simonetti, A.; Burns, P. C., Time-resolved self-assembly of a fullerene-topology core-shell cluster containing 68 uranyl polyhedra. *J. Am. Chem. Soc.* **2012,** *134*, 1810-1816.
(15) Ling, J.; Qiu, J.; Burns, P. C., Uranyl peroxide oxalate cage and core-shell clusters containing 50 and 120 uranyl ions. *Inorg. Chem.* **2012,** *51*, 2403-2408.
(16) Ling, J.; Ozga, M.; Stoffer, M.; Burns, P. C., Uranyl peroxide pyrophosphate cage clusters with oxalate and nitrate bridges. *Dalton Trans.* **2012,** *41*, 7278-7284.
(17) Unruh, D. K.; Ling, J.; Qiu, J.; Pressprich, L.; Baranay, M.; Ward, M.; Burns, P. C., Complex nanoscale cage clusters built from uranyl polyhedra and phosphate tetrahedra. *Inorg. Chem.* **2011,** *50*, 5509-5516.
(18) Ling, J.; Qiu, J.; Szymanowski, J. E. S.; Burns, P. C., Low-symmetry uranyl pyrophosphate cage clusters. *Chem.-Eur. J.* **2011,** *17*, 2571-2574.

(19) Ling, J.; Qiu, J.; Sigmon, G.; Ward, M.; Szymanowski, J. E. S.; Burns, P. C., Uranium pyrophosphate/methylenediphosphonate polyoxometalate cage clusters. *J. Am. Chem. Soc.* **2010,** *132*, 13395-13402.
(20) Sigmon, G. E.; Ling, J.; Unruh, D. K.; Moore-Shay, L.; Ward, M.; Weaver, B.; Burns, P. C., Uranyl-peroxide interactions favor nanocluster self-assembly. *J. Am. Chem. Soc.* **2009,** *131*, 16648-16649.
(21) Qiu, J.; Kevin, N.; Jouffret, L.; Szymanowski, J. E. S.; Burns, P. C., Time-resolved assembly of chiral uranyl peroxo cage clusters containing belts of polyhedra. *Inorg. Chem.* **2013,** *52*, 337-345.
(22) Miro, P.; Pierrefixe, S.; Gicquel, M.; Gil, A.; Bo, C., On the origin of the cation templated self-assembly of uranyl-peroxide nanoclusters. *J. Am. Chem. Soc.* **2010,** *132*, 17787-17794.
(23) Miro, P.; Vlaisavljevich, B.; Gil, A.; Burns, P. C.; Nyman, M.; Bo, C., Self-assembly of uranyl-peroxide nanocapsules in basic peroxidic environments. *Chem.-Eur. J.* **2016,** *22*, 8571-8578.
(24) Dembowski, M.; Olds, T. A.; Pellegrini, K. L.; Hoffmann, C.; Wang, X. P.; Hickam, S.; He, J. H.; Oliver, A. G.; Burns, P. C., Solution ^{31}P NMR study of the acid-catalyzed formation of a highly charged {$U(_{24})Pp(_{12})$} nanocluster, $[(UO_2)_{24}(O_2)_{24}(P_2O_7)_{12}]^{48-}$, and its structural characterization in the solid state using single-crystal neutron diffraction. *J. Am. Chem. Soc.* **2016,** *138*, 8547-8553.
(25) Blanchard, F.; Ellart, M.; Rivenet, M.; Vigier, N.; Hablot, I.; Morel, B.; Grandjean, S.; Abraham, F., Role of ammonium ions in the formation of ammonium uranyl peroxides and uranyl peroxo-oxalates. *Cryst. Growth Des.* **2016,** *16*, 200-209.
(26) Meca, S.; Marti, V.; De Pablo, J.; Giménez, J.; Casas, I., UO_2 dissolution in the presence of hydrogen peroxide at pH > 11. *Radiochim. Acta* **2008,** *96*, 535-539.
(27) Peper, S. M.; Brodnax, L.; Field, S.; Zehnder, R.; Valdez, S.; Runde, W., Kinetic study of the oxidative dissolution of UO_2 in aqueous carbonate media. *Ind. Eng. Chem. Res.* **2004,** *43*, 8188-8193.
(28) Kim, K. W.; Chung, D. Y.; Yang, H. B.; Lim, J. K.; Lee, E. H.; Song, K. C.; Song, K., A conceptual process study for recovery of uranium alone from spent nuclear fuel by using high-alkaline carbonate media. *Nucl. Technol.* **2009,** *166*, 170-179.
(29) Armstrong, C. R.; Nyman, M.; Shvareva, T.; Sigmon, G. E.; Burns, P. C.; Navrotsky, A., Uranyl peroxide enhanced nuclear fuel corrosion in seawater. *Proc. Natl. Acad. Sci. U.S.A.* **2012,** *109*, 1874-1877.
(30) Burns, P. C.; Ewing, R. C.; Navrotsky, A., Nuclear fuel in a reactor accident. *Science* **2012,** *335*, 1184-1188.
(31) McNamara, B.; Buck, E.; Hanson, B., Observation of studtite and metastudtite on spent fuel. In *Scientific Basis for Nuclear Waste Management Xxvi*, Finch, R. J.; Bullen, D. B., Eds. Materials Research Society: Warrendale, 2003; Vol. 757, pp 401-406.
(32) Makenas, B. J. W. H., Analysis of sludge from K East basin floor and weasel pit - WHC-SP--1182. Westinghouse Hanford Co., Richland, WA (United States) Sponsoring Organization: USDOE Office of Environmental Restoration and Waste Management, Washington, DC (United States): 1996.

(33) Zanonato, P. L.; Di Bernardo, P.; Grenthe, I., A calorimetric study of the hydrolysis and peroxide complex formation of the uranyl(VI) ion. *Dalton Trans.* **2014,** *43*, 2378-2383.
(34) Burns, P.C.; Nyman, M., Captivation with encapsulation: a dozen years of exploring uranyl peroxide capsules. *Dalton Trans. 47*, 5916-5927.
(35) Mizuno, N.; Nakajima, H.; Tanaka, H.; Kudo, T., Novel formation of nitrate and ammonium ions by reaction of inorganic molybdenum nitride with hydrogen peroxide, *Chem. Lett.* **1997**, *26*, 521-522.
(36) Nakajima, H.; Kudo, T.; Mizuno, N., Reaction of metal, carbide, and nitride of tungsten with hydrogen peroxide characterized by ^{183}W nuclear magnetic resonance and Raman spectroscopy. *Chem. Mater.* **1999**, *11*, 691-697.
(37) McGrail, B. T.; Sigmon, G. E.; Jouffret, L. J.; Andrews, C. R.; Burns, P. C., Raman spectroscopic and ESI-MS characterization of uranyl peroxide cage clusters. *Inorg. Chem.* **2014,** *53*, 1562-1569.
(38) Dembowski, M.; Bernales, V.; Qiu, J.; Hickam, S.; Gaspar, G.; Gagliardi, L.; Burns, P. C., Computationally-guided assignment of unexpected signals in the Raman spectra of uranyl triperoxide complexes. *Inorg. Chem.* **2017,** *56*, 1574-1580.
(39) Kubatko, K. A.; Forbes, T. Z.; Klingensmith, A. L.; Burns, P. C., Expanding the crystal chemistry of uranyl peroxides: synthesis and structures of di- and triperoxodioxouranium(VI) complexes. *Inorg. Chem.* **2007,** *46*, 3657-3662.

For Table of Contents Only

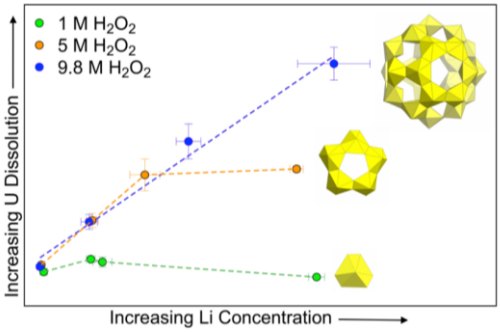

UN and UO_2 readily dissolve in solutions containing hydrogen peroxide and alkali hydroxide to form uranyl peroxide species. Resulting uranium concentrations and uranyl speciation in solution are dependent on H_2O_2 and alkali concentrations. In solutions containing higher concentrations of H_2O_2, uranyl peroxide cage clusters form and the U concentration in solution depends on alkali availability. When H_2O_2 concentrations are lower, high alkali concentrations lead to formation of smaller uranyl peroxide species and lower U solution concentrations.